Available online at www.sciencedirect.com
ScienceDirect
Journal of Solid State Chemistry 180 (2007) 2525–2533
JOURNAL OF SOLID STATE CHEMISTRY
www.elsevier.com/locate/jssc

Short-time hydrothermal synthesis and delamination of ion exchangeable Mg/Ga layered double hydroxides

Ugur Unal*

Department of Nano Science and Technology, Faculty of Engineering, Kumamoto University, Kurokami 2-39-1, Kumamoto 860-8555, Japan

Received 19 April 2007; received in revised form 10 July 2007; accepted 10 July 2007
Available online 13 July 2007

Abstract

The hydrothermal synthesis of magnesium–gallium layered double hydroxides (Mg/Ga LDHs) was studied under static and agitated conditions. Not only well-crystallized and large-sized Mg/Ga LDHs having hexagonal morphology were obtained but also the reaction time was comparatively decreased from 24 to 2 h by means of agitation during hydrothermal synthesis. In static conditions, mainly GaOOH and magnesite phases were formed. The elemental analysis results show that the final Mg/Ga ratio is significantly different from the initial ratio. The reason was attributed to the difference in the hydrolytic behavior of Mg^{2+} and Ga^{3+}. Furthermore, the anion exchange studies with glycine, dodecyl sulfate, ferrocyanide and ferricyanide were performed to investigate the intercalation behavior of the anions into Mg/Ga LDHs. In addition, delamination of Mg/Ga LDHs was performed in formamide for the glycine exchanged forms. Large size of nanosheets thus obtained can be utilized in the fabrication of functional thin films.

Keywords: Layered double hydroxide; Hydrothermal synthesis; Crystallization; Ion exchange; Delamination

1. Introduction

Layered double hydroxides are hydrotalcite-like layered compounds composed of piled-up positively charged brucite-like layers and charge balancing anions as well as water molecules in the interlayer domain. The general formula of layered double hydroxides is represented by $[M^{2}_{1-x}+M^{3+}_{x}(OH)_2]^{q+}\,[A^{n-}_{x/n}\cdot mH_2O]$, where M^{2+} and M^{3+} are divalent and trivalent metal cations, and A is *n*-valent interlayer guest anion, which might be Cl^-, CO_3^{2-}, NO_3^-, OH^-, etc. [1]. The positive charge of the layer, which is resulted from the partial displacement of divalent cations with trivalent ones, is compensated by the interlayer anions. LDHs are known to have good anion exchange capacity and a wide range of molecules can be introduced into the interlayer for many purposes. In addition, LDHs have a wide range of applications such as anion exchangers [2], catalyst supports [3], bioactive nanocomposites [4–6], and electroactive materials [7–9]. The properties and applications of LDHs have been well summarized in various reviews [2,10–12] and a book chapter [13].

LDHs can generally be prepared by precipitation of the corresponding divalent and trivalent cations in an alkali solution [13–15]. Direct synthesis of LDHs involves the precipitation of divalent and trivalent metal cations in a concentrated NaOH solution. The synthesis of LDHs can be carried out in a similar way under constant pH, where NaOH solution and a solution of cations are added into the reaction chamber slowly and steadily under vigorous stirring, so that cations are co-precipitated simultaneously at a regulated pH value. These processes generally provide aggregated LDH crystallites with poor crystallinity. Thus, further treatment (aging) of the resultant slurry at a higher temperature to obtain well-crystallized LDHs might be needed. In general, hydrothermal treatment is applied for the purpose. In another method, one can obtain LDH crystallites after slow and homogenous precipitation of metal cations as a result of the slow hydrolysis of urea at a certain temperature and aging for a long period of time at elevated temperatures [16,17]. The preparation techniques

*Fax: +81 96 342 3679.
E-mail address: ugurunal@chem.kumamoto-u.ac.jp

0022-4596/$ - see front matter © 2007 Elsevier Inc. All rights reserved.
doi:10.1016/j.jssc.2007.07.005

were explained in detail in different reviews, and book chapters [10,13–15]. Recently, hexamethylenetetramine was introduced as an alternative hydrolysis agent to replace urea [18]. It is known that slow hydrolysis in the presence of urea or HMTA gives better-crystallized LDHs with high aspect ratio [17–20].

Hydrothermal synthesis is a well-known and established method. It is used as a post-synthesis treatment to improve the crystallinity of the products of above-mentioned techniques or a stand-alone technique to obtain well-crystallized LDH phases [13–15,19,20]. Heating the reactants in a pressurized aqueous media improves the crystallinity of the resultant LDH and particle size but required time might be a day or longer under static conditions. The crystallization of LDHs is highly affected by synthesis temperature and time. There are a few reports on the time dependence of crystallization with hydrothermal treatment or other methods [17,21,22]. In this study, we have showed that if the synthesis of Mg/Ga LDH is performed at high temperatures under agitation, the period can be reduced to a relatively shorter synthesis time.

As mentioned, a high content of guest anions in LDHs results in strong interlayer electrostatic interactions, which make it difficult to delaminate via normal procedures. On the other hand, delamination is a necessary process for the construction of two-dimensional single sheets [23]. The first study of delamination was reported for a dodecylsulfate intercalated LDH that delaminates under refluxing with butanol at 120 °C for 16 h [23,24]. Delamination of dodecylsulfate-intercalated LDHs in a polar acrylate monomer at 70 °C with shearing [25], delamination of LDHs containing glycine in the interlayer with formamide [26,27], and delamination of lactate containing LDHs in water [28] are other routes to obtain nanosize sheets of layered double hydroxides. Recently, Sasaki et al. reported delamination of various Cl^- and NO_3^- exchanged LDHs in formamide [29–31].

In this study, we have reported the synthesis and crystallization of Mg/Ga LDH in agitated hydrothermal conditions. It is well known that LDHs composed of especially Mg^{2+}, Zn^{2+}, Co^{2+}, Al^{3+} gives high crystallinity with large size of LDH sheets under appropriate reaction conditions. In this study, we have replaced Al^{3+} with Ga^{3+} in a widely studied Mg/Al LDH system, as Ga^{3+} is known to have a similar hydrolytic behavior to Al^{3+}. Although there are a number of reports on the Mg/Ga system [32–36], it, to our knowledge, has not been examined for its hydrothermal synthesis. The anion exchange experiments of the LDH were performed with glycine, dodecylsulfate, ferricyanide and ferrocyanide and delamination of Mg/Ga LDHs in formamide could be achieved for the glycine exchanged form. The LDH nanosize sheets can be promising materials for the application in several fields such as photoluminescence [37], photochemistry [38] and electrochemistry [39] like layered metal oxide materials.

2. Experimental section

2.1. Synthesis

$Mg(NO_3)_2 \cdot 6H_2O$ (Wako, Ltd.), $Ga(NO_3)_3 \cdot xH_2O$ ($7 < x < 9$) (Wako, Ltd.) and hexamethylenetetramine (HMT) (Wako, Ltd.) were used as starting materials for the synthesis of Mg/Ga LDHs. The reactants were used as received. Hydrothermal method was utilized for the synthesis of Mg/Ga LDHs in this study. The reaction was performed in either an air sealed teflon reactor (SUS 316), which works in static conditions or an stainless steel reactor (Akico Co., Japan) mounted with a shaker. Hereafter the former and the latter reactor will be referred as TR and SR, respectively. After filling 50% capacity of reactors, TR was simply placed in an oven set at desired temperature and SR was fixed into a shaker unit of the heating device and temperature was set at desired temperature. The unit was shaken at 60 rpm. Another third reactor (Taiatsu Techno Co., Japan), which will be referred as TL, was also used for the synthesis of the LDH. The reactor contains Teflon lined stainless steel part equipped with a stirring unit and a heating jacket. The reactor volume capacity is 100 ml and it was filled ca. 50% of its capacity. The Teflon part coupled to a mechanical stirring unit was heated at 150 °C for 1 day. Stirring rate was 300 rpm. The agitation condition for each reactor was listed in Table 1.

The Mg:Ga:HMT molar ratio in the starting solution was adjusted to 3:1:3. The aqueous mixture of $Mg(NO_3)_2 \cdot 6H_2O$ and $Ga(NO_3)_3 \cdot xH_2O$ (x was estimated as 7.7 according to ICP results) was added to an aqueous solution of HMT so that the final molar ratios will be equal to 0.3, 0.1 and 0.3 M, respectively. Freshly decarbonated Milli-Q water ($R > 18\ M\Omega\,cm$ and TOC = 12 ppb) was used throughout the experiments. The product was filtered and washed with substantial amount of decarbonated water and dried at 40 °C for 1 day in an oven. The synthesis conditions for TR, SR and TL were given in Table 1.

2.2. Salt-acid treatment and ion-exchange reactions

The salt-acid treatment [40] was carried out to remove the carbonate anions from the interlayer domain of LDHs with using a solution containing 1.5 M NaCl and 4 mM HCl. 0.1 g of LDH powder was stirred in the salt-acid solution for 24 h and recovered by filtering. The ion-exchanged LDH

Table 1
The synthesis and agitation conditions of Mg/Ga LDHs in three types of reactor

Reactor	Condition	Reaction temperatures (°C)	Time (h)
TR	Static	120, 150, 170	24
SR	Shaken	150, 170, 200	2, 6, 10
TL	Stirred	150	24

was rinsed with a copious amount of water and dried in an oven at 40 °C overnight.

Ion exchange reactions with various molecules were accomplished as follows: 20 mg of Cl^- exchanged LDH was stirred in 40 ml solution containing 0.2 M ferricyanide, ferrocyanide, dodecylsulfate or glycine for 48 h. After the reaction was complete, the solution was filtered and washed with a copius amount of decarbonated water. Ion exchanged LDHs were dried at 40 °C for 1 day in an oven.

2.3. Delamination

Delamination of LDHs was carried out by following the route proposed by Hibino [27]. Ten milligram of glycine exchanged LDH was shaken in 20 ml formamide for 2 days. Prior to the addition of LDH powder, formamide was purged with N_2 gas. The delamination reaction was performed in a sample bottle, which was tightly closed after filling with N_2 gas. After 2 days, the colloidal delamination solution was centrifuged at 2000 rpm for 10 min to remove the particles that are not delaminated.

2.4. Characterization

The crystal structure and the orientation were analyzed from XRD patterns (using Cu$K\alpha$ radiation, Rigaku RINT-2500VHF) of LDH powders. The morphology was examined with a scanning electron microscopy (SEM, JEOL). The compositions were analyzed with an ICP spectrophotometer (Nippon Jarrel Ash IRIS Advantage), CHN analysis and the energy dispersive X-ray spectroscopy (EDX) attached to SEM. Infrared spectra of the LDH powders before and after ion exchange reactions were analyzed with a Fourier transform infrared spectrometer (FTIR, Perkin Elmer). KBr pellet technique was used for the analyses of LDH powders. A certain amount of a sample was mixed with KBr in a ratio of 2:100 w/w and pressed into a pellet. Atomic force microscopy (Nanoscope, Digital Instruments) was used to obtain AFM images of the surface topography of the LDH nanosheets on a Mica substrate. A fresh surface of Mica substrate was obtained by removing outer layers and the substrate was dipped into a delamination solution of LDH and held for 10 min. Then, rinsed with a copious amount of water and dried under N_2 gas stream.

3. Results and discussion

3.1. Synthesis

Fig. 1 gives the XRD patterns of hydrothermally synthesized Mg/Ga LDHs at different temperatures in TR in static conditions for 24 h. The reaction in TR, regardless of the reaction temperature, produced a mixture of different phases that are mainly LDH structure, gallium oxide hydrate (GaOOH) phase and a minor amount of magnesite phase. As seen in the figure, based on the fact

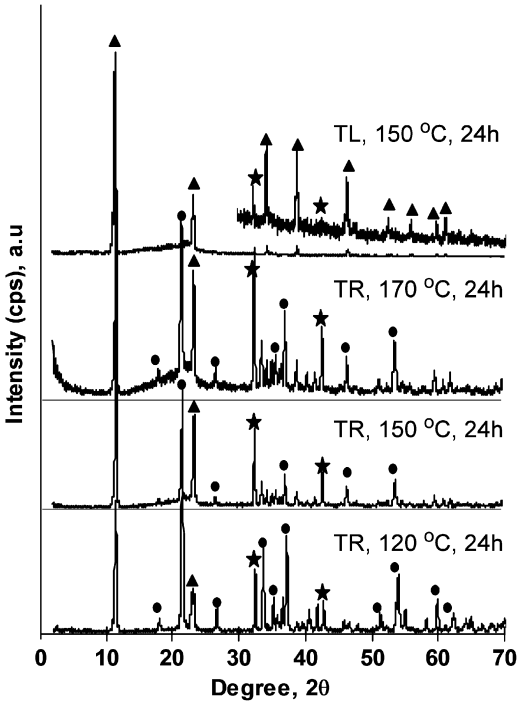

Fig. 1. XRD patterns of LDHs prepared in TR at 120 °C, 24 h; 150 °C, 24 h; 170 °C, 24 h and in TL at 150 °C, 24 h, respectively, from bottom to top. Triangles shows main LDH peaks, full circles are for GaOOH peaks and star represents magnesite peaks.

that intensity of LDH related peaks increases and that of other phases diminishes at higher synthesis temperatures, increasing the temperature promotes the formation of LDH phase. This trend is supported by the SEM micrographs. Mainly a unique rod-like GaOOH phase was observed for the samples synthesized at 120 °C in TR (Fig. 2a), but LDH and magnesite phases appeared at 150 and 170 °C in TR with more intense peaks on the XRD patterns in Fig. 1 and also became more visible on the SEM pictures as seen in Fig. 2b. The SEM image, which is well consistent with the XRD pattern of the sample prepared in TR at 150 °C, 24 h (Fig. 1), shows the formation of rod-like structure, which is GaOOH phase [41,42] and also cubic $MgCO_3$ (magnesite, marked with stars in Fig. 1 and with the circles in Fig. 2) phase together with the well-crystallized hexagonal LDHs slabs having a lateral size of 10–15 μm. Increasing the temperature promotes the formation of LDH phases but apparently does not help getting rid of GaOOH and magnesite phases in static conditions. The EDX spectrum of the sample prepared in TR at 150 °C for 24 h in Fig. 3 confirms that the rod-like morphology is formed mainly from gallium and oxygen, thus indicating that these structures could be GaOOH. The in-figure SEM micrograph shows the GaOOH-rich region of the sample on which EDX analysis was carried out. On the other hand, pure LDH phases could be obtained in SR at 6 h treatment in agitated conditions depending on the synthesis temperature as seen in Fig. 4. The figure gives the XRD patterns of Mg/Ga LDHs synthesized in SR at

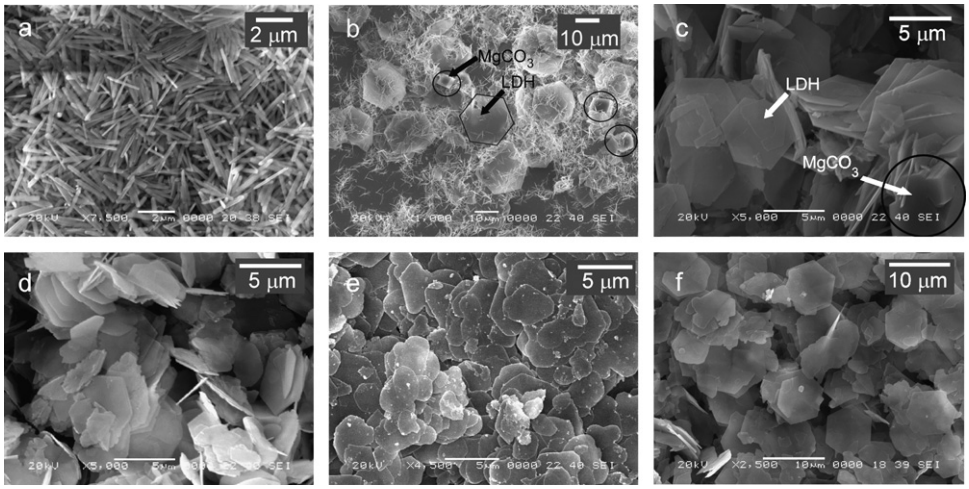

Fig. 2. SEM pictures of samples synthesized at various conditions: (a) TR, 120 °C, 24 h; (b) TR, 150 °C, 24 h; (c) SR, 150 °C, 6 h; (d) SR, 170 °C, 6 h; (e) SR, 200 °C, 6 h and (f) TL, 150 °C, 24 h. Magnesite phase was circled on the figures. Hexagonal and plate-like structures are LDH phase and rod-like structures represent GaOOH phase.

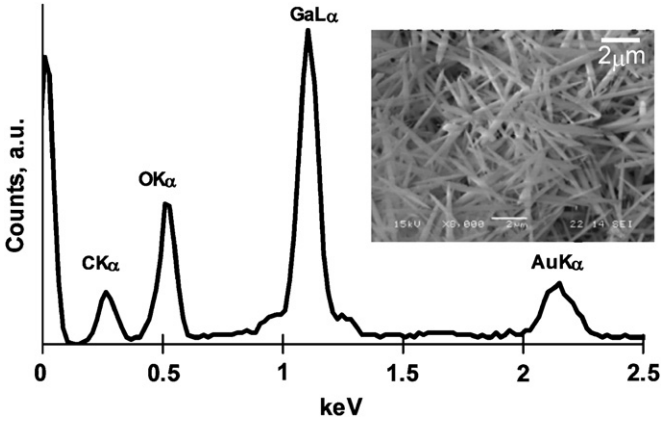

Fig. 3. The EDX spectrum of the GaOOH phase observed in the sample prepared in TR at 150°C for 24 h. The in-figure SEM micrograph shows the GaOOH-rich region of the sample.

various temperatures for 6 h. These XRD patterns show characteristic sharp and symmetric LDH peaks at lower 2θ values and less intense peaks at higher angles.

XRD patterns of the Mg/Ga LDHs synthesized in SR in agitated conditions at various temperatures demonstrate highly crystallized single LDH phase in a relatively short reaction time. We could obtain highly crystalline LDH phase after hydrothermal reaction under agitation even at 200 °C for 2 h (result not shown). As given in Fig. 4, LDH prepared in SR at 150 °C for 6 h possesses some minor magnesite impurity, which is also visible as shown with an arrow and circled on the SEM image given in Fig. 2c but the XRD patterns of the samples prepared at 170 and 200 °C (Fig. 4) give the characteristic diffraction peaks of the LDH phase only. A hump centered around 20° was also observed on the XRD patterns of the samples prepared in SR at 150 and 170 °C for 6 h in Fig. 4. This hump can be attributed to the presence of amorphous gallium or magnesium phases. When the reaction time for the samples prepared in SR increased to 10 h, some slight

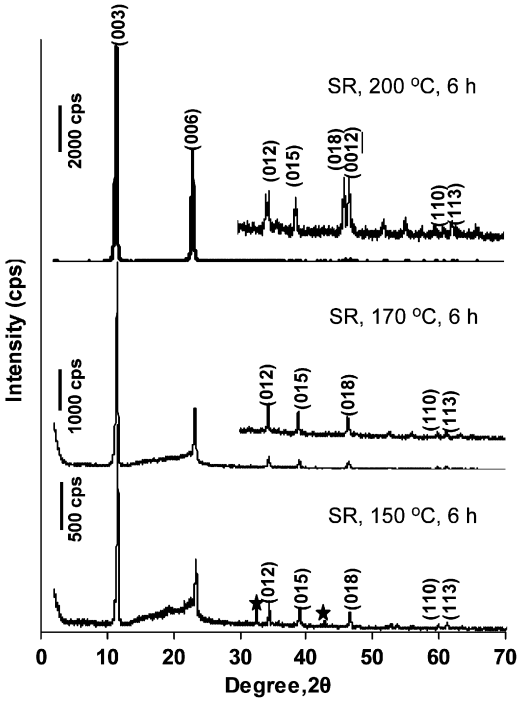

Fig. 4. XRD patterns of LDHs synthesized in SR at 150 °C, 6 h; 170 °C, 6 h and 200 °C, 6 h, from bottom to top. Star show the magnesite phase.

phases appeared on the XRD patterns as given in Fig. 5. The figure shows the XRD patterns of the samples prepared in SR at three different temperatures for 10 h. The longer time treatment developed slight magnesite phase in the samples prepared in SR at 150 and 170 °C for 10 h. On the other hand, the weak peak at around 30° on the XRD pattern of the sample prepared at 200 °C for 10 h given in the Fig. 5 shows the presence of Ga_2O_3. These slight phases might be crystallized from the amorphous gallium or magnesium hydroxides.

SEM micrographs of the LDHs prepared in SR at 150 and 170 °C for 6 h show that LDH crystals are quite large

with a lateral size of around 5 μm (Figs. 2c and d, respectively). The XRD patterns of these LDHs give sharper peaks in response to increasing temperature and the morphology of the particles changes dramatically as shown in Fig. 2e. At lower temperatures, LDHs having regular hexagonal shapes were discerned (Figs. 2c and d) while they were constituted by irregular platelet shapes at higher temperatures (Fig. 2e). The unit cell parameters of LDHs were given in Table 2, which tabulates the final Mg/Ga ratio, *d* value, structural parameters and thickness in *c* direction for LDHs. XRD patterns of the LDH phases and these values are in quite good agreement with typical LDH crystallized in 3R1 polytype [43]. The crystallite size in *c* direction given in the table was calculated by using Scherrer's formula and FWHM values estimated for the (003) peaks on the XRD patterns. The FWHM value for (003) peak was estimated as 0.28 for the sample synthesized in SR at 170 °C for 6 h and the value was reduced to 0.22 for the sample prepared in SR at 200 °C for 6 h. FWHM value remained the same when the reaction time for the sample prepared in SR at 200 °C was increased to 10 h. According to this fact, we can conclude that the crystallinity increases with increasing temperature. The above data also show that the increase in the crystallinity of the LDH phase is temperature-dependent rather than time-dependent, which actually is in agreement with the same observation reported by previous studies [21].

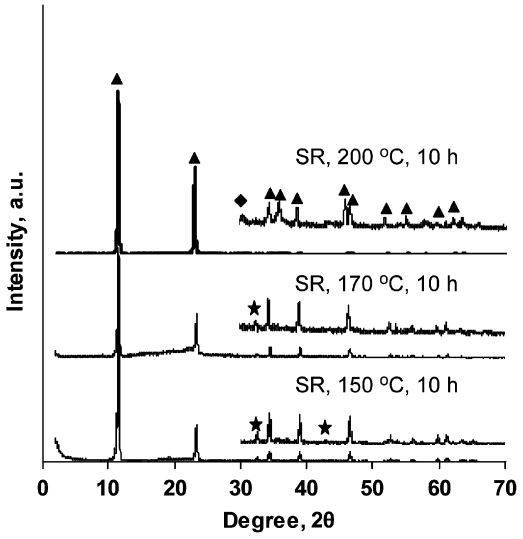

Fig. 5. XRD patterns of LDHs synthesized in SR at 150 °C, 10 h; 170 °C, 10 h and 200 °C, 10 h, from bottom to top. Triangles shows main LDH peaks, star show the magnesite phase and Ga_2O_3 phase was marked with a filled diamond.

The LDHs were prepared also in TL at 150 °C for 24 h to observe the effect of stirring, which was successful to remove GaOOH while magnesite phase is still available as seen in the XRD pattern of the sample given in Fig. 1. The SEM image given in Fig. 2f shows the well-crystallized LDH slabs under stirring. Another observation made from SEM micrographs is that stirring or shaking worked in favor of the reduced particle sizes. The above data show that the crystallization of the LDHs is affected by temperature and agitation of the reaction media. The compositions of the cubic (magnesite) and plate-like hexagonal morphologies observed in the SEM micrograph of the LDH prepared in TL under stirring were confirmed by EDX analyses. As seen in Fig. 6a, EDX spectrum of the cubic structure possesses mainly Mg, C, and O peaks, which indicates that the morphology belongs to the magnesite structure marked with a circle in Fig. 6b. On the other hand, the EDX spectrum of the LDH slabs in Fig. 6c gives Mg, Ga, O and C peaks as expected. The Mg/Ga atomic ratio for the sample estimated by EDX analysis is slightly lower than the value estimated from ICP results. The estimated value from the EDX data is 2.21 for the sample. ICP results for the same sample, on the other hand, give the value of 2.33 as seen in Table 2. The difference might be as a result of the slight presence of the $MgCO_3$ phase in the sample, which affects the ICP results.

Elemental analysis of the synthesized LDHs shows that the final Mg/Ga ratio in the products is lower than the initial ratio in the mixture placed in the reactor (see Table 2). When $Ga(NO_3)_3$ was titrated with an alkali solution, the $Ga(NO_3)_3$ solution results in a turbid solution in the pH range 3.7–9.7. In this range, gallium exist in its insoluble hydroxide forms like GaOOH or $Ga(OH)_3$ [42,44]. However, gallium hydroxide species are quite soluble at alkali environment and it produces soluble alkali salts at low pH values [42]. For Mg^{2+}, on the other hand, true hydroxide formation condition occurs over pH 10 [16,32]. GaOOH formation takes place between the pH values of 6–8 according to the literature [42]. The initial pH value of the starting Mg^{2+}/Ga^{3+}/HMT mixture was measured around 4, which is high enough for the formation of gallium hydroxide species according to the titration curve of $Ga(NO_3)_3$ and the related studies [42,44]. We have measured the pH of the solution around 7.5 after the hydrothermal reaction was complete. This value is high enough for the formation of gallium

Table 2
Final Mg/Ga Ratio, *d* value, structural parameters and thickness of a crystallite in *c* direction for LDHs

Reaction condition	Final Mg/Ga ratio	*d* Value (Å)	Structural parameters (Å)		Thickness in *c* direction (Å)
			a	*c*	
SR, 170 °C, 6 h	1.79	7.63	3.0839	22.89	51.98
SR, 200 °C, 6 h	2.37	7.72	3.0952	23.16	66.15
TL, 150 °C, 24 h	2.33	7.64	3.0877	22.92	55.93

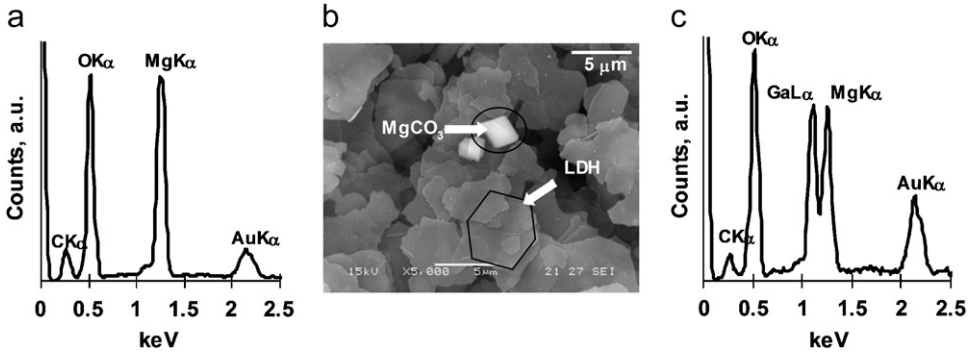

Fig. 6. (a) EDX spectrum of the cubic phase ($MgCO_3$) circled in the (b) SEM micrograph and (c) EDX spectrum of the hexagonal phase (LDH) marked in the (b) SEM micrograph.

hydroxide species but $Mg(OH)_2$ is fairly soluble in this pH range, in which the hydrothermal reaction takes place. In addition, the elemental analysis after the filtration of the reaction mass revealed a substantial amount of Mg^{2+} in the filtrate together with trace amount of Ga^{3+}. Consequently, not all Mg^{2+} can incorporate into the LDH layer and as a result, final Mg/Ga ratio is less than the initial stoichiometric ratio. The result is consistent with previous reports in most of which the final Mg/Ga ratio differs from the initial one [32,34,35,45].

The comparison of the SEM pictures and XRD patterns of the sample prepared in SR at 170 °C for 6 h (Figs. 2d and 4) and the sample prepared in TR at 170 °C for 24 h (Fig. 1, SEM image not shown but similar to Fig. 2b) clearly reveals that the agitation of the reaction media has an obvious effect on the crystallinity and quality of the final product. It has been well known that trivalent metals precipitate initially below pH = 10 and then divalent species in the reaction solution react with these precursors [32,45,46]. The probable mechanism in the static conditions is that readily formed gallium hydroxide species may act as precursors to GaOOH species [42,44,47]. In static conditions, the diffusion between the precursor hydroxide species in the reactor is unfavorable and as a result, a mixture of GaOOH, $MgCO_3$ and, depending on the temperature, LDH slabs is formed in the reactor. On the other hand, agitation of the reaction media promotes the diffusion of Mg^{2+} species into the gallium hydroxide species in the solution and induces mixing at higher atomic level. In this case, gallium hydroxide species are the primary particles for the crystal growth of LDHs. LDH crystals start to grow around these primary particles with the diffusion of Mg^{2+} under agitation. Consequently, pure LDH phases could be obtained under agitation at optimum reaction temperature and time for the current system because of the favorable diffusion conditions in the reactor in favor of the formation of LDH phases only.

3.2. Decarbonation and intercalation behavior

LDHs are known to have a very high affinity to carbonate and the presence of carbonate in the interlayer

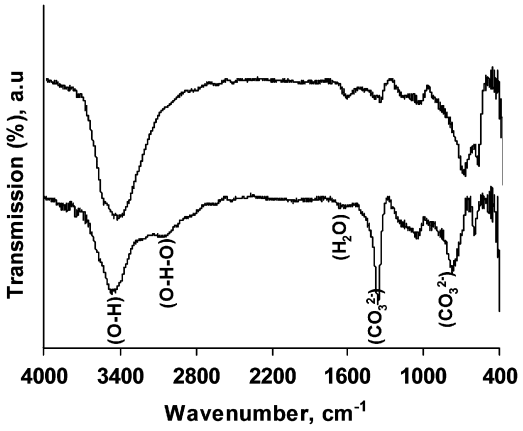

Fig. 7. FTIR spectra of LDH prepared in TL at 150 °C, 24 h before (bottom figure) and after Cl^- exchange (top figure) reaction.

of LDHs is an obstacle to ion exchange and delamination of LDHs. If carbonates in the interlayer can be replaced by another anion such as Cl^- or NO_3^-, intercalation of larger anionic molecules or delamination of LDHs can be easily achieved. Iyi et al. [40] reported a method for the decarbonation of LDHs. The method is called salt-acid treatment and involves the treatment of LDHs with an aqueous mixture of a salt at high concentration and its corresponding acid in a diluted amount. In this study, 0.1 g LDHs was treated with 1.5 M NaCl and 4 mM HCl in 100 ml H_2O. Fig. 7 shows the FTIR spectra of the as prepared Mg/Ga LDH in the TL and of the decarbonated form in the region 400–4000 cm^{-1}. LDH indicates an intense peak at 1356 cm^{-1} associated with CO_3^{2-}. Another peak at around 750 cm^{-1} also suggest the bending mode of CO_3^{2-} and it overlaps with M–O (metal–oxygen) vibration modes. After the salt-acid treatment, however, M–O stretching and vibration bands become dominant. The broad peak at 3450 cm^{-1} can be assigned to O–H stretching mode of the interlayer water and hydrogen stretching mode of OH group. The shoulder of the peak at 3040 cm^{-1}, which disappears after salt-acid treatment is due to the H-bonded water molecules to CO_3^{2-}. In the case of salt-acid treated sample, a weak peak of CO_3^{2-} reveals that unexchanged CO_3^{2-} is still existed in the interlayer domain.

The ion exchange experiments were performed for LDHs prepared in TL under stirring. Dodecyl sulfate, ferricyanide, ferrocyanide and glycine were used to investigate the intercalation behavior of Mg/Ga LDHs. Fig. 8 shows the XRD patterns of LDHs intercalated with several anions. The main diffraction peak shifted to lower angles after ion exchange reaction with these anions, which is indicating the intercalation of anions into the interlayer. Dodecylsulfate intercalated LDH has a basal spacing of 25.08 Å, which indicates that dodecylsulfate, of which molecular length is 21.3 Å was oriented perpendicularly [48]. In addition to the XRD patterns, FTIR spectra (Fig. 9a) confirms the presence of dodecylsulfate anions in the interlayer domain. Based on the XRD patterns, ferrocyanide and ferricyanide intercalated LDHs have a basal spacing of 10.46 Å and 11.01 Å, respectively. The basal spacings indicate, according to many reports regarding the intercalated structure, that the cyanide complexes are placed in the interlayer with their 3-fold axis perpendicular to the host layer. It was also mentioned that this orientation is preferable for this kind of complexes [49]. There is a slight difference in the basal spacing between LDHs intercalated with two anions having cyano groups probably because of the structural difference in the interlayer The difference might be as a result of the fact that the ferrocyanide ion is known to have a smaller radius (4.33 Å) than that of ferricyanide ion (4.45 Å) [50]. The XRD pattern of the glycine exchanged LDH was also given in Fig. 8. The *d* value of 7.75 Å for the sample is slightly smaller than those reported by previous reports probably due to the different hydration state of the anion in the interlayer of the LDH.

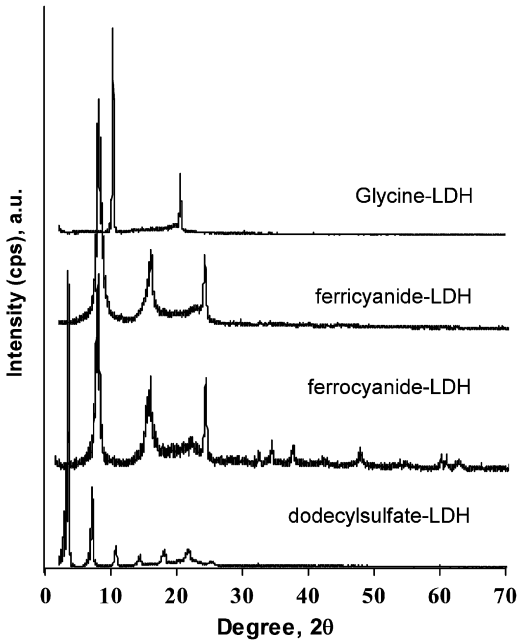

Fig. 8. XRD patterns of dodecylsulfate, ferrocyanide, ferricyanide and glycine exchanged LDH prepared in TL at 150 °C, 24 h, respectively, from bottom to top.

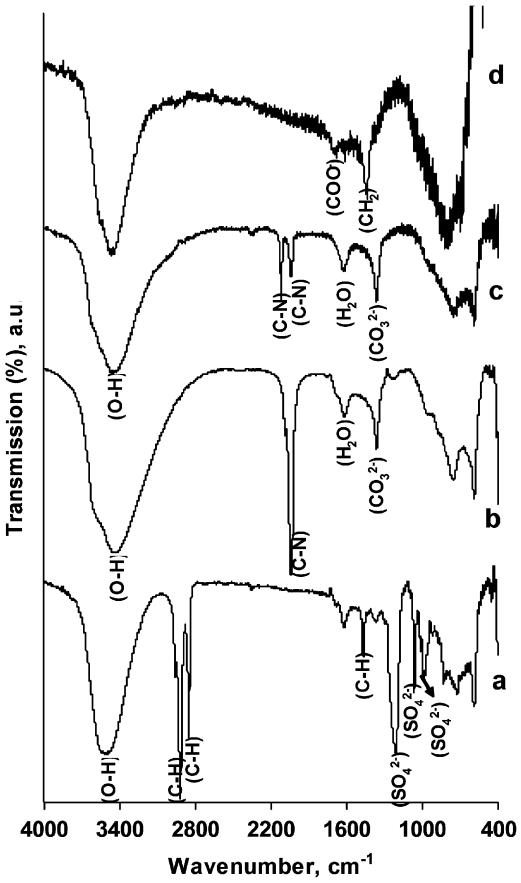

Fig. 9. FTIR spectra of: (a) dodecylsulfate, (b) ferrocyanide, (c) ferricyanide and (d) glycine exchanged LDH synthesized in TL at 150 °C, 24 h.

As shown in Fig. 9a, the dodecylsulfate incorporated LDH shows sharp bands on the FTIR spectra in the range of 950–1250 cm^{-1}. These bands are due to the stretching mode of sulfate, while stretching vibrations of CH_2 in the alkyl chain of dodecylsulfate are at 2851 and 2918 cm^{-1} [48,51,52]. The band at 1468 cm^{-1} is assigned to the bending mode of CH_2. In spectrum 9b, which represents the ferrocyanide intercalated LDH, stretching mode of CN has a maximum absorption at 2038 cm^{-1}. This behavior is similar to the spectra of ferrocyanide molecule in an aqueous solution, of which C–N stretching mode gives a band at 2038 cm^{-1} [53]. These data show that ferrocyanide in the interlayer of the LDH keeps its original ionic structure. The FTIR spectrum of ferricyanide intercalated LDH gives a sharp peak at 2118 cm^{-1} due to the stretching mode of CN (Fig. 9c), which was assigned to the intercalated ferricyanide anion based on the fact that its aqueous solution gives the corresponding peak around 2110 cm^{-1} [49]. On the other hand, appearance of ferrocyanide related peak at 2034 cm^{-1} on the spectrum of ferricyanide intercalated sample suggests that both cyanide forms of the complex molecule coexist in the interlayer of the ferricyanide intercalated LDH. The existence of ferrocyanide in the ferricyanide intercalated LDH is as a result of the partial reduction of ferricyanide

during intercalation [49,50,54,55]. There are several reports on the similar behavior of ferricyanide anions in the interlayer of LDHs. It was discussed by Idemura et al. and several other authors that the plastic deformation as a result of the stress applied on ferricyanide anions by the host layer results in the reduction of ferricyanide to ferrocyanide [50]. This plastic deformation was believed to occur during the preparation of pellets for FTIR analysis, where pressure is applied to form KBr-sample pellets. Fernandez et al. [56] however, showed the similar reduction behavior with diffure reflectance infrared Fourier spectroscopy (DRIFT), which requires no pressure for sample preparation. This finding was supported by the report of Carpani et al. [57] in which IR spectra was performed with ATR. However, it is agreed that the reduction is based on the stress in the interlayer molecules applied by the host layer. Fig. 9d shows the FTIR spectra of the glycine exchanged LDH. The bands at 1358 and 1591 cm^{-1} can be attributable to the glycinate ion in the interlayer [58]. On FTIR spectra of the intercalated samples, we have also observed a band of CO_3^{2-} at ~1360 cm^{-1}. The band appears more intensely on the spectrum of the ferrocyanide-exchanged sample. These data show that CO_3^{2-} also coexists in the interlayer of the intercalated LDHs.

3.3. Delamination of Mg/Ga LDHs

It is well known that delamination has an important role to obtain nanostructured materials [23–31]. However, delamination of LDHs is difficult because of the high charge density of the LDH layers, dense network of hydrated interlayer anions and the large particle size of LDHs. Several methods have been developed to delaminate LDHs. Among them, the method that includes delamination of LDHs in polar formamide solvent described by Hibino et al. [26,27] is beneficial without any heating and refluxing treatment. According to that method, glycine exchanged Mg/Ga LDH is dispersed in formamide at room temperature to get translucent colloidal solution after centrifugation. The AFM image of nanosheets of the LDH synthesized in TL at 150 °C for 24 h is given in Fig. 10 and shows that the delamination with formamide was successful for Mg/Ga LDHs. The theoretical thickness of an LDH layer is 0.48 nm [27] and the observed average thickness of 0.8 nm for the delaminated sheets is in a good agreement with the theoretical thickness. The deviation might be as a result of the adsorption of formamide molecules onto the surface of the sheets. As seen in the figure, the original hexagonal shape of the LDHs is lost after the delamination process. This is as a result of the cracking and breakage of very thin layers of the LDH during the delamination process. A small bright particle can be also observed on the AFM image. The particle might be very small unexfoliated particle adsorbed on the surface of the nanosheet.

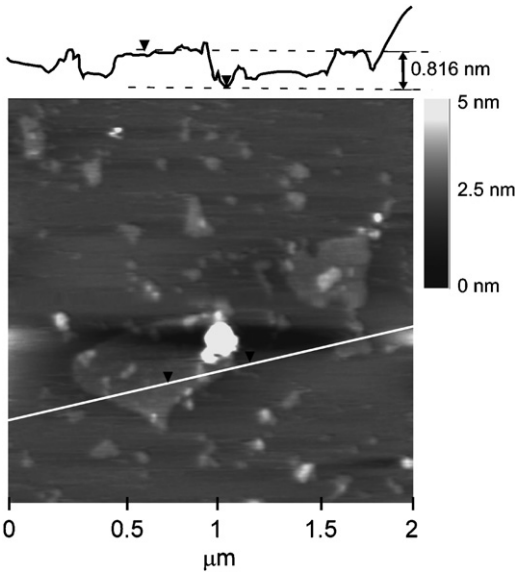

Fig. 10. AFM picture of the LDH nanosheets delaminated from the LDH synthesized at 150 °C, 24 h.

4. Conclusions

In summary, the hydrothermal reaction of Mg^{2+} and Ga^{3+} in the presence of HMT resulted in mainly GaOOH phases in static conditions. Increasing the reaction temperature, however, helped carrying the reaction path to the formation of LDH structures but it was only possible to obtain pure LDH phase after applying agitation to the reaction media, moreover, in shorter reaction times. Under agitation, increasing the temperature also helped obtaining well-crystallized LDH structures. Agitation provides better diffusion conditions in the reaction media and as a result readily available Ga^{3+} species at the reaction pH can react with Mg^{2+} species to give pure LDH phase as a product. However, the stoichiometric ratio does not match the initial ratio because of the difference in the hydrolytic behavior of Ga^{3+} and Mg^{2+} species in the reaction pH. We have also showed that LDHs can be ion exchanged with different anions and can be delaminated into single nanosize sheets. As a potential source to nanosize sheets, LDHs can find a range of application in various fields such as electrochemistry or photoluminescence, which is currently under investigation.

Acknowledgments

I am grateful to Prof. Yasumichi Matsumoto for his support and making the publication of this study possible. I would also like to thank Ms. Ozge Altuntasoglu for her help in doing the experiments and to Dr. Shintaro Ida for his discussions. The EDX analyses were kindly carried out by Dr. Takateru Yamamuro at Department of Materials Science and Engineering, Kumamoto University. This work was supported by The Grant-in-Aid for Japan

Society for the Promotion of Science (JSPS) fellows (No. 17 · 05413).

References

[1] S. Miyata, Clays Clay Miner. 23 (1975) 369.
[2] S.P. Newman, W. Jones, New J. Chem. (1998) 105.
[3] S. Hamada, K. Ikeue, M. Machida, Chem. Mater. 17 (2005) 4873.
[4] J.H. Choy, S.Y. Kwak, J.S. Park, Y.J. Jeong, J. Portier, J. Am. Chem. Soc. 121 (1999) 1399.
[5] J.H. Choy, S.Y. Kwak, Y.J. Jeong, J.S. Park, Angew. Chem. Int. Ed. 39 (2000) 4042.
[6] J.H. Choy, S.Y. Kwak, J.S. Park, Y.J. Jeong, J. Mater. Chem. 11 (2001) 1671.
[7] J. Tronto, K.C. Sanchez, E.L. Crepaldi, Z. Naal, S.I. Klein, J.B. Valim, J. Phys. Chem. Sol. 65 (2004) 493.
[8] B. Mavis, M. Akinc, J. Power Sources 134 (2004) 308.
[9] J. Qiu, G. Villemure, J. Electroanal. Chem. 428 (1997) 165.
[10] D.G. Evans, X. Duan, Chem. Commun. (2006) 485.
[11] A.I. Khan, D. O'Hare, J. Mater. Chem. 12 (2002) 3191.
[12] F. Leroux, J.P. Besse, Chem. Mater. 13 (2001) 3507.
[13] P.S. Braterman, Z.P. Xu, F. Yarberry, in: S.M. Auerbach, K.A. Carrado, P.K. Dutta (Eds.), Handbook of Layered Materials, Marcel Dekker, Inc., New York, 2004 p. 373.
[14] A. de Roy, C. Forano, J.P. Besse, in: V. Rives (Ed.), Layered Double Hydroxides: Present and Future, Nova Science Publishers, New York, 2001 p. 1.
[15] J. He, M. Wei, B. Li, Y. Kang, D.G. Evans, X. Duan, Struct. Bond. 119 (2006) 89.
[16] U. Costantino, F. Marmottini, M. Nocchetti, R. Vivani, Eur. J. Inorg. Chem. (1998) 1439.
[17] J.M. Oh, S.H. Hwang, J.H. Choy, Solid State Ionics 151 (2002) 285.
[18] N. Iyi, T. Matsumoto, Y. Kaneko, K. Kitamura, Chem. Lett. 33 (2004) 1122.
[19] M. Ogawa, H. Kaiho, Langmuir 18 (2002) 4240.
[20] M.M. Rao, B.R. Reddy, M. Jayalakshmi, V.S. Jaya, B. Sridhar, Mater. Res. Bull. 40 (2005) 347.
[21] F. Kovanda, D. Kolousek, Z. Cilova, V. Hulinsky, Appl. Clay Sci. 28 (2005) 101.
[22] S. Kannan, R.V. Jasra, J. Mater. Chem. 10 (2000) 2311.
[23] M. Adachi-Pagano, C. Forano, J.P. Besse, Chem. Commun. (2000) 91.
[24] F. Leroux, M. Adachi-Pagano, M. Intissar, S. Chauviere, C. Forano, J.P. Besse, J. Mater. Chem. 11 (2001) 105.
[25] S. O'Leary, D. O'Hare, G. Seeley, Chem. Commun. (2002) 1506.
[26] T. Hibino, W. Jones, J. Mater. Chem. 11 (2001) 1321.
[27] T. Hibino, Chem. Mater. 16 (2004) 5482.
[28] T. Hibino, M. Kobayashi, J. Mater. Chem. 15 (2005) 653.
[29] L. Li, R. Ma, Y. Ebina, N. Iyi, T. Sasaki, Chem. Mater. 17 (2005) 4386.
[30] Z. Liu, R. Ma, M. Osada, N. Iyi, Y. Ebina, K. Takada, T. Sasaki, J. Am. Chem. Soc. 128 (2006) 4872.
[31] Z. Liu, R. Ma, Y. Ebina, N. Iyi, K. Takada, T. Sasaki, Langmuir 23 (2007) 861.
[32] M.R. Weir, J. Moore, R.A. Kydd, Chem. Mater. 9 (1997) 1686.
[33] B. Rebours, J.B. d'Espinose de la Caillarie, O.J. Clause, J. Am. Chem. Soc. 116 (1994) 1707.
[34] E. Lopez-Salinas, M. Garcia-Sanchez, M.A.L. Ramon-Garcia, I. Schifter, J. Porous Mater. 3 (1996) 169.
[35] M.A. Aramendia, V. Borau, C. Jimenez, J.M. Marinas, F.J. Romero, J.R. Ruiz, J. Solid State Chem. 131 (1997) 78.
[36] M.A. Aramendia, Y. Aviles, V. Borau, J.M. Luque, J.M. Marinas, J.R. Ruiz, F.J. Urbano, J. Mater. Chem. 9 (1999) 1603.
[37] Y. Matsumoto, U. Unal, Y. Kimura, S. Ohashi, K. Izawa, J. Phys. Chem. B 109 (2005) 12748.
[38] K. Izawa, T. Yamada, U. Unal, S. Ida, O. Altuntasoglu, M. Koinuma, Y. Matsumoto, J. Phys. Chem. B 110 (2006) 4645.
[39] U. Unal, S. Ida, K. Shimogawa, O. Altuntasoglu, K. Izawa, C. Ogata, T. Inoue, Y. Matsumoto, J. Electroanal. Chem. 595 (2006) 95.
[40] N. Iyi, T. Matsumoto, Y. Kaneko, K. Kitamura, Chem. Mater. 16 (2004) 2926.
[41] X. Liu, G. Qiu, Y. Zhao, N. Zhang, R. Yi, J. Alloy Compd. 439 (2007) 275.
[42] J. Zhang, Z. Liu, C. Lin, J. Lin, J. Crystal Growth 280 (2005) 99.
[43] V.A. Drifts, A.S. Bookin, in: V. Rives (Ed.), Layered Double Hydroxides: Present and Future, Nova Science Publishers, New York, 2001 p. 39.
[44] A.C. Tas, P.J. Majewski, F. Aldinger, J. Am. Ceram. Soc. 85 (2002) 1421.
[45] E. Lopez-Salinas, E. Torres-Garcia, M. Garcia-Sanchez, J. Phys. Chem. Solids 58 (1997) 919.
[46] G. Defontaine, L.J. Michot, I. Bihannic, J. Ghanbaja, V. Briois, Langmuir 20 (2004) 9834.
[47] S. Avivi, Y. Mastai, G. Hodes, A. Gedanken, J. Am. Chem. Soc. 121 (1999) 4196.
[48] Y. Guo, H. Zhang, L. Zhao, G.D. Li, J.S. Chen, L. Xu, J. Solid State Chem. 178 (2005) 1830.
[49] J.W. Boclair, P.S. Braterman, B.D. Brister, Z. Wang, F. Yarberry, J. Solid State Chem. 161 (2001) 249.
[50] S. Idemura, E. Suzuki, Y. Ono, Clays Clay Miner. 37 (1989) 553.
[51] A. Clearfield, M. Kieke, J. Kwan, J.L. Colon, R.C. Wang, J. Incl. Phenom. Mol. Recog. Chem. 11 (1991) 361.
[52] J.T. Rajamathi, N. Ravishankar, M. Rajamathi, Solid State Sci. 7 (2005) 195.
[53] H.C.B. Hansen, C.B. Koch, Clays Clay Miner. 42 (1994) 179.
[54] M.J. Holgado, V. Rives, M.S. Sanroman, P. Malet, Solid State Ionics 92 (1996) 273.
[55] R.L. Frost, A.W. Musumeci, J. Bouzaid, M.O. Adebajo, W.N. Martens, J.T. Kloprogge, J. Solid State Chem. 178 (2005) 1940.
[56] J.M. Fernandez, M.A. Ulibarri, F.M. Labajos, V. Rives, J. Mater. Chem. 8 (1998) 2507.
[57] I. Carpani, M. Berrettoni, M. Giorgetti, D. Tonelli, J. Phys. Chem. B 110 (2006) 7265.
[58] F. Wypych, G.A. Bubniak, M. Halma, S. Nakagaki, J. Colloid Interface Sci. 264 (2003) 203.